

Adaptive Passivity-based Synchronization of Spatiotemporal Neural Networks with Multi-weighted Coupling under Spatially Point Measurements

Haoyun Tang¹, Haodong Cui¹, Mingyu Ma¹, Cheng Hu^{1,2}, and Tingting Shi¹

¹ College of Mathematics and System Science, Xinjiang University, Urumqi 830017, China,

² Xinjiang Key Laboratory of Applied Mathematics(XJDX1401), Urumqi 830017, China

`hucheng@xju.edu.cn`.

Abstract. This article focuses on the adaptive synchronization of spatiotemporal neural networks with multi-weighted coupling based on the theory of passivity. Firstly, based on the spatial point measurements, an innovative adaptive spatial sampling controller is developed. Subsequently, by utilizing variable rearrangement technique and passivity theory, several passivity and passivity-based synchronization criteria are derived for system with mismatched input and output dimensions. Moreover, the weighted union matrices of all coupling layers are assumed to be irreducible, which relaxes the previous requirements for each coupling matrix. Finally, a numerical example is presented to validate the effectiveness of the obtained results.

Keywords: Coupled neural network, Adaptive spatial sampling control, Passivity and synchronization, Multiweighted coupling

1 Introduction

Coupled neural networks (CNNs) have attracted considerable attention due to their ability to integrate intrinsic node dynamics with complex network behaviors. This unique characteristic has enabled their successful applications in various domains, including secure communication, image recognition, and signal processing. Notably, many real-world systems, such as social, email, and transportation networks, can be effectively modeled as multi-weighted CNNs [1], where each node is associated with multiple weights. For instance, individuals can interact through platforms such as Instagram, Facebook and Twitter, illustrating the multi-weighted nature of network couplings. Compared to single-weighted models, multi-weighted networks provide a more detailed representation of interrelationships [2], making their study both valuable and promising.

Furthermore, reaction-diffusion equations, a fundamental class of partial differential equations, describe the spatial propagation of information and play a

crucial role in various practical applications. As a result, the dynamic behaviors of reaction-diffusion neural networks have attracted widespread research interest in recent years [3]. By incorporating reaction-diffusion mechanisms into multi-weighted CNNs, researchers can gain a more comprehensive understanding of network dynamics, thereby expanding their potential applications [4]. Such models are widely used in biological pattern formation, neural activity modeling, and image processing.

Passivity and synchronization are two critical dynamical behaviors in multi-weighted coupled reaction-diffusion neural networks. Passivity, a fundamental concept originally introduced by Bevelevich in circuit analysis [5], is a special case of dissipativity. In a passive system, the energy stored is always less than the energy supplied externally over a given period [6], ensuring that the system cannot generate energy independently but only dissipates externally provided energy, thereby guaranteeing internal stability. Due to its widespread applications in mechanical systems, power networks, and various other fields, the study of passivity in multi-weighted CNNs with reaction-diffusion term has attracted growing attention. For instance, Wang et al. [7] investigated passivity in multi-adaptive coupled fractional-order reaction-diffusion neural networks. The event-triggered passivity problem of multi-weighted coupled reaction-diffusion memristive neural networks was addressed by Huang et al. in [8]. Furthermore, by reformulating the synchronization problem as an error system stability analysis with input and output, passivity provides an effective framework for addressing synchronization challenges. Wang [9] established synchronization criteria for multiple-derivative coupled reaction-diffusion neural networks based on the relationship between output-strict passivity and synchronization. Additionally, by leveraging output-strict passivity, Wang et al. [10] achieved synchronization in multi-weighted coupled neural networks.

Since multi-weighted CNNs usually do not exhibit passivity on their own, some control strategies are required to ensure their passivity. These strategies include impulsive control [11], pinning control [12], and feedback control [13]. To prevent the issue of excessive gain during control, this paper introduces adaptive control to achieve passivity and synchronization. Adaptive control, an important control technique, has been widely employed in multi-weighted CNNs in recent years [14,15]. Yang et al. [14] proposed an edge-based adaptive control strategy to achieve finite-time passivity and finite-time synchronization of coupled fractional-order memristive neural networks with multi-state couplings. Wang et al. [15] employed node- and edge-based adaptive event-triggered control to address the lag outer synchronization of multi-weighted CNNs. It is worth noting that all the above results impose adaptive control on the full domain. However, in practical applications, the complete full domain information is often not available, so this paper introduces adaptive sampling control, which has better applicability.

Inspired by the above, this article explores the passivity-based synchronization of spatiotemporal neural networks with multi-weighted coupling via adaptive spatial sampling controller. A spatiotemporal neural network with multi-

weighted coupling is first constructed. Secondly, an adaptive spatial sampling controller is proposed, which dynamically updates the control gain and is more cost-effective and convenient than full-domain control [16]. Based on Lyapunov method and passivity theory, several passivity and passivity-based synchronization criteria are derived for the multi-weighted spatiotemporal neural networks. Specially, the strong irreducibility requirement of each coupling layer in [17] is relaxed to the irreducibility of the weighted union matrices in light of the variable rearrangement technique.

Notations: $\mathcal{R}_{\geq 0}$ represents $[0, \infty]$, matrix $\mathcal{W} > 0$ indicates that \mathcal{W} is positive definite. \mathcal{W}^T is the transpose of \mathcal{W} . $[\mathcal{W}]^s = \frac{\mathcal{W}^T + \mathcal{W}}{2}$. $\lambda_{\min}(\mathcal{W})$ is the minimum eigenvalue of \mathcal{W} . $\text{diag}\{\cdot\}$ is a diagonal matrix. For any vector $v = (v_1, v_2, \dots, v_n)^T \in \mathcal{R}^n$, $\|v\|_2 = (\sum_{i=1}^n v_i^2)^{\frac{1}{2}}$. For any $\varphi(t, \vartheta) = (\varphi_1(t, \vartheta), \varphi_2(t, \vartheta), \dots, \varphi_n(t, \vartheta)) \in \mathcal{R}^n$, $\|\varphi(t, \vartheta)\|_{[a,b]} = (\int_a^b \sum_{\ell=1}^n \varphi_\ell^2(t, \vartheta) d\vartheta)^{\frac{1}{2}}$.

2 Preparation and Problem Formation

Consider a kind of spatiotemporal neural networks with σ -weighted couplings, which is represented by

$$\begin{aligned} \frac{\partial \varphi_i(t, \vartheta)}{\partial t} = & \mathcal{D} \frac{\partial^2 \varphi_i(t, \vartheta)}{\partial \vartheta^2} - \mathcal{A} \varphi_i(t, \vartheta) + \mathcal{B} f(\varphi_i(t, \vartheta)) \\ & + \sum_{\eta=1}^{\sigma} \sum_{j=1}^N c^\eta g_{ij}^\eta \Gamma^\eta \varphi_j(t, \vartheta) + \mathcal{I}_i(t, \vartheta) + u_i(t, \vartheta), \end{aligned} \quad (1)$$

where $(t, \vartheta) \in \mathcal{R}_{\geq 0} \times (a, b)$, $i \in \overline{1, N}$, $\varphi_i(t, \vartheta) = (\varphi_i^1(t, \vartheta), \varphi_i^2(t, \vartheta), \dots, \varphi_i^n(t, \vartheta))^T \in \mathcal{R}^n$ is the state of the i -th neural network, $f(\varphi_i(t, \vartheta)) = (f^1(\varphi_i^1(t, \vartheta)), f^2(\varphi_i^2(t, \vartheta)), \dots, f^n(\varphi_i^n(t, \vartheta)))^T$ is the nonlinear activation function, $\mathcal{I}_i(t, \vartheta) \in \mathcal{R}^n$ represents the external input, $u_i(t, \vartheta) \in \mathcal{R}^n$ is an adaptive spatial sampling controller. $\mathcal{D} = \text{diag}\{d_1, d_2, \dots, d_n\} > 0$ is the diffusion coefficient matrix, $\mathcal{A} = \text{diag}\{a_1, a_2, \dots, a_n\}$, $a_\ell > 0$ denotes the potential decay rate of the ℓ -th neuron toward its resting state, $\mathcal{B} = (b_{ij})_{n \times n}$ is the synaptic connection weight matrix, $c^\eta > 0$ and $\Gamma^\eta = \text{diag}\{\gamma_1^\eta, \gamma_2^\eta, \dots, \gamma_n^\eta\} > 0$ are the coupling strength and the inner coupling matrix of the η -th coupling, $\mathcal{G}^\eta = (g_{ij}^\eta)_{N \times N}$ is the outer coupling matrix of the η -th coupling, where $g_{ij}^\eta > 0$ ($i \neq j$) indicates a direct link from the node j to the node i , and $g_{ii}^\eta = -\sum_{j=1, j \neq i}^N g_{ij}^\eta$.

The Dirichlet boundary condition and the initial state of system (1) are given by

$$\begin{cases} \varphi_i(t, a) = \varphi_i(t, b) = \mathbf{0}_n, \\ \varphi_i(0, \vartheta) = \phi_i(\vartheta), \end{cases} \quad (2)$$

where $\phi_i(\vartheta) = (\phi_i^1(\vartheta), \phi_i^2(\vartheta), \dots, \phi_i^n(\vartheta))^T \in \mathcal{R}^n$ ($i \in \overline{1, N}$) is the continuous initial value function.

Assumption 1. For all $\varphi, \varphi^* \in \mathbb{R}^n$, there exists a constant $L \geq 0$ such that the nonlinear function $f(\cdot) : \mathbb{R}^n \rightarrow \mathbb{R}^n$ satisfies

$$\|f(\varphi) - f(\varphi^*)\|_2 \leq \sqrt{L}\|\varphi - \varphi^*\|_2.$$

Assumption 2. For any $\ell \in \overline{1, n}$, $\mathcal{G}^{(\ell)}$ is irreducible, where $\mathcal{G}^{(\ell)} = \sum_{\eta=1}^{\sigma} c^{\eta} \gamma_{\ell}^{\eta} \mathcal{G}^{\eta}$.

Remark 1. In [17], each coupling matrix is assumed to be irreducible, which implies that the corresponding communication topology is strongly connected. Notably, this paper relaxes that assumption by requiring only the irreducibility of the weighted union matrix formed by all coupling layers. This weaker condition ensures that the overall communication topology, represented by the union matrix, remains strongly connected.

Under Assumption 1, the matrix $\mathcal{G}^{(\ell)}$ has a simple zero eigenvalue, and there exists a vector $\xi^{(\ell)} = (\xi_1^{\ell}, \xi_2^{\ell}, \dots, \xi_N^{\ell})^T \in \mathcal{R}^N$ with $\xi_m^{\ell} > 0$ ($m \in \overline{1, N}$) such that $(\mathcal{G}^{(\ell)})^T \xi^{(\ell)} = \mathbf{0}_N$ and $\sum_{i=1}^N \xi_i^{\ell} = 1$. Based on $\xi^{(\ell)}$, the target is defined as

$$\bar{\varphi}^{\ell}(t, \vartheta) = \sum_{m=1}^N \xi_m^{\ell} \varphi_m^{\ell}(t, \vartheta), \quad (t, \vartheta) \in \mathcal{R}_{\geq 0} \times (a, b),$$

where $\bar{\varphi}^{\ell}(t, \vartheta) \in \mathcal{R}$, $\ell \in \overline{1, n}$.

Define $\varsigma_i^{\ell}(t, \vartheta) = \varphi_i^{\ell}(t, \vartheta) - \bar{\varphi}^{\ell}(t, \vartheta) \in \mathcal{R}$. From equations (1) and $\mathcal{G}^{(\ell)T} \xi^{(\ell)} = \mathbf{0}_N$, one obtains

$$\begin{aligned} \frac{\partial \varsigma_i^{\ell}(t, \vartheta)}{\partial t} &= d_{\ell} \frac{\partial^2 \varsigma_i^{\ell}(t, \vartheta)}{\partial \vartheta^2} - a_{\ell} \varsigma_i^{\ell}(t, \vartheta) \\ &+ \sum_{s=1}^n b_{\ell s} f^s(\varphi_i^s(t, \vartheta)) - \sum_{m=1}^N \xi_m^{\ell} \sum_{s=1}^n b_{\ell s} f^s(\varphi_m^s(t, \vartheta)) \\ &+ \mathcal{I}_i^{\ell}(t, \vartheta) - \sum_{m=1}^N \xi_m^{\ell} \mathcal{I}_m^{\ell}(t, \vartheta) + u_i^{\ell}(t, \vartheta) - \sum_{m=1}^N \xi_m^{\ell} u_m^{\ell}(t, \vartheta) \\ &+ \sum_{\eta=1}^{\sigma} \sum_{j=1}^N c^{\eta} g_{ij}^{\eta} \gamma_{\ell}^{\eta} \varphi_j^{\ell}(t, \vartheta), \quad i \in \overline{1, N}, \ell \in \overline{1, n}. \end{aligned} \quad (3)$$

To explore the passivity of system (3), its output is given by

$$y_i(t, \vartheta) = P \varsigma_i(t, \vartheta) + Q \bar{\mathcal{I}}_i(t, \vartheta), \quad i \in \overline{1, N}, \quad (4)$$

where $y_i(t, \vartheta) = (y_i^1(t, \vartheta), \dots, y_i^p(t, \vartheta))^T \in \mathcal{R}^p$, $\varsigma_i(t, \vartheta) = (\varsigma_i^1(t, \vartheta), \dots, \varsigma_i^n(t, \vartheta))^T \in \mathcal{R}^n$, $\bar{\mathcal{I}}_i(t, \vartheta) = (\bar{\mathcal{I}}_i^1(t, \vartheta), \dots, \bar{\mathcal{I}}_i^n(t, \vartheta))^T \in \mathcal{R}^n$, $\bar{\mathcal{I}}_i^{\ell}(t, \vartheta) = \mathcal{I}_i^{\ell}(t, \vartheta) - \sum_{m=1}^N \xi_m^{\ell} \mathcal{I}_m^{\ell}(t, \vartheta)$, and $P, Q \in \mathcal{R}^{p \times n}$.

Denote

$$\begin{aligned} \hat{\mathcal{I}}(t, \vartheta) &= \left((\hat{\mathcal{I}}^{(1)}(t, \vartheta))^T, (\hat{\mathcal{I}}^{(2)}(t, \vartheta))^T, \dots, (\hat{\mathcal{I}}^{(n)}(t, \vartheta))^T \right)^T \in \mathcal{R}^{nN}, \\ \hat{\mathcal{I}}^{(\ell)}(t, \vartheta) &= (\bar{\mathcal{I}}_1^{\ell}(t, \vartheta), \bar{\mathcal{I}}_2^{\ell}(t, \vartheta), \dots, \bar{\mathcal{I}}_N^{\ell}(t, \vartheta))^T \in \mathcal{R}^N, \end{aligned}$$

$$\begin{aligned}\hat{\mathcal{O}}(t, \vartheta) &= \left((\mathcal{O}^{(1)}(t, \vartheta))^T, (\mathcal{O}^{(2)}(t, \vartheta))^T, \dots, (\mathcal{O}^{(n)}(t, \vartheta))^T \right)^T \in \mathcal{R}^{pN}, \\ \mathcal{O}^{(\ell)}(t, \vartheta) &= (y_1^\ell(t, \vartheta), y_2^\ell(t, \vartheta), \dots, y_N^\ell(t, \vartheta))^T \in \mathcal{R}^N.\end{aligned}$$

Definition 1 [16]. System (3) with input vector $\hat{\mathcal{I}}(t, \vartheta) \in \mathcal{R}^{nN}$ and output vector $\hat{\mathcal{O}}(t, \vartheta) \in \mathcal{R}^{pN}$ is said to be strictly passive if there exist a storage function $W(t)$ and matrices $\mathcal{H} \in \mathcal{R}^{pN \times nN}$, $0 < \mathcal{H}_1 \in \mathcal{R}^{nN \times nN}$, and $0 < \mathcal{H}_2 \in \mathcal{R}^{pN \times pN}$ such that for any $t \in \mathcal{R}_{\geq 0}$, $\hat{\psi}_1(t) \geq 0$. Besides, system (3) is output-strictly passive (input-strictly passive) if $\hat{\psi}_2(t) \geq 0$ ($\hat{\psi}_3(t) \geq 0$), where

$$\begin{aligned}\hat{\psi}_1(t) &= \int_a^b \hat{\mathcal{O}}^T(t, \vartheta) \mathcal{H} \hat{\mathcal{I}}(t, \vartheta) d\vartheta - \int_a^b \hat{\mathcal{I}}^T(t, \vartheta) \mathcal{H}_1 \hat{\mathcal{I}}(t, \vartheta) d\vartheta - \int_a^b \hat{\mathcal{O}}^T(t, \vartheta) \mathcal{H}_2 \hat{\mathcal{O}}(t, \vartheta) d\vartheta - \dot{W}(t), \\ \hat{\psi}_2(t) &= \int_a^b \hat{\mathcal{O}}^T(t, \vartheta) \mathcal{H} \hat{\mathcal{I}}(t, \vartheta) d\vartheta - \int_a^b \hat{\mathcal{O}}^T(t, \vartheta) \mathcal{H}_1 \hat{\mathcal{O}}(t, \vartheta) d\vartheta - \dot{W}(t), \\ \hat{\psi}_3(t) &= \int_a^b \hat{\mathcal{O}}^T(t, \vartheta) \mathcal{H} \hat{\mathcal{I}}(t, \vartheta) d\vartheta - \int_a^b \hat{\mathcal{I}}^T(t, \vartheta) \mathcal{H}_2 \hat{\mathcal{I}}(t, \vartheta) d\vartheta - \dot{W}(t).\end{aligned}$$

Lemma 1[18]. For any scalar $\varepsilon > 0$ and vectors $\alpha, \beta \in \mathcal{R}^n$,

$$2\alpha^T \beta \leq \varepsilon \alpha^T \alpha + \varepsilon^{-1} \beta^T \beta.$$

Lemma 2[19]. Given a square-integrable vector function $\varphi : [a, b] \rightarrow \mathcal{R}^n$ satisfies $\varphi(a) = 0$ or $\varphi(b) = 0$, and a matrix $0 < \mathcal{M} \in \mathcal{R}^{n \times n}$. Then,

$$\int_a^b \varphi(\xi)^T \mathcal{M} \varphi(\xi) d\xi \leq \frac{4(b-a)^2}{\pi^2} \int_a^b \left(\frac{d\varphi}{d\xi} \right)^T \mathcal{M} \left(\frac{d\varphi}{d\xi} \right) d\xi.$$

Moreover, if $\varphi(a) = \varphi(b) = 0$, then

$$\int_a^b \varphi(\xi)^T \mathcal{M} \varphi(\xi) d\xi \leq \frac{(b-a)^2}{\pi^2} \int_a^b \left(\frac{d\varphi}{d\xi} \right)^T \mathcal{M} \left(\frac{d\varphi}{d\xi} \right) d\xi.$$

3 Main results

In this section, the passivity and synchronization of spatiotemporal neural networks will be analyzed by designing adaptive spatial sampling controller. For convenience, define

$$\begin{aligned}\mathcal{P} &= P \otimes \mathbf{I}_N, \quad \mathcal{Q} = Q \otimes \mathbf{I}_N, \quad \Lambda^{(\ell)} = \text{diag}\{\xi_1^\ell, \xi_2^\ell, \dots, \xi_N^\ell\}, \\ \Lambda &= \text{diag}\{\Lambda^{(1)}, \Lambda^{(2)}, \dots, \Lambda^{(n)}\} \in \mathcal{R}^{nN \times nN}.\end{aligned}$$

A set of fixed points ϑ_p is chosen such that $a = \vartheta_0 < \vartheta_1 < \dots < \vartheta_{m-1} < \vartheta_m = b$, $[\vartheta_p, \vartheta_{p+1})$ is the sampling interval and $\bar{\vartheta}_p = \frac{\vartheta_p + \vartheta_{p+1}}{2}$ is sampling point. Assume that $\sup_{p \in \{0, m-1\}} \{\vartheta_{p+1} - \vartheta_p\} = \delta > 0$.

The adaptive spatial sampling control controller is formulated as

$$\begin{cases} u_i^\ell(t, \vartheta) = -\kappa_i(t, \vartheta) \varsigma_i^\ell(t, \bar{\vartheta}_p), & \vartheta \in [\vartheta_p, \vartheta_{p+1}), p \in \overline{0, m-1}, \\ \frac{\partial \kappa_i(t, \vartheta)}{\partial t} = \sum_{\ell=1}^n \theta_i \xi_i^\ell \varsigma_i^\ell(t, \vartheta) \varsigma_i^\ell(t, \bar{\vartheta}_p), & \vartheta \in [\vartheta_p, \vartheta_{p+1}), p \in \overline{0, m-1}. \end{cases} \quad (5)$$

where $\kappa_i(0, \vartheta) \geq 0$, $i \in \overline{1, N}$, $\ell \in \overline{1, n}$. Denote $\kappa = \mathbf{I}_n \otimes \text{diag}\{\kappa_1, \kappa_2, \dots, \kappa_N\} \geq 0$.

3.1 Passivity

Theorem 1. Under Assumptions 1-2 and adaptive spatial sampling controller (5), there exist matrices $\mathcal{H} \in \mathcal{R}^{pN \times nN}$, $0 < \mathcal{H}_1 \in \mathcal{R}^{nN \times nN}$, and $0 < \mathcal{H}_2 \in \mathcal{R}^{pN \times pN}$ such that system (3) is strictly passive.

Proof. Pick a Lyapunov function

$$W(t) = U(t) + \sum_{i=1}^N \frac{1}{2\theta_i} \int_a^b (\kappa_i(t, \vartheta) - \kappa_i^*)^2 d\vartheta, \quad (6)$$

and

$$U(t) = \frac{1}{2} \sum_{\ell=1}^n \int_a^b (\varsigma^{(\ell)}(t, \vartheta))^T \Lambda^{(\ell)} \varsigma^{(\ell)}(t, \vartheta) d\vartheta,$$

where $t \in \mathcal{R}_{\geq 0}$, $\varsigma^{(\ell)} = (\varsigma_1^\ell(t, \vartheta), \dots, \varsigma_N^\ell(t, \vartheta))^T \in \mathbb{R}^N$, $\ell \in \overline{1, n}$, $\hat{\varsigma}(t, \vartheta) = ((\varsigma^{(1)}(t, \vartheta))^T, (\varsigma^{(2)}(t, \vartheta))^T, \dots, (\varsigma^{(n)}(t, \vartheta))^T)^T \in \mathbb{R}^{nN}$, $\kappa_i^* > 0$.

Take the derivative to $W(t)$ along error system (3),

$$\begin{aligned} \dot{W}(t) &= \sum_{i=1}^N \sum_{\ell=1}^n \int_a^b \xi_i^\ell \varsigma_i^\ell(t, \vartheta) \left[d_\ell \frac{\partial^2 \varsigma_i^\ell(t, \vartheta)}{\partial \vartheta^2} - a_\ell \varsigma_i^\ell(t, \vartheta) \right. \\ &\quad + \sum_{s=1}^n b_{\ell s} f^s(\varphi_i^s(t, \vartheta)) - \sum_{s=1}^n b_{\ell s} f^s(\bar{\varphi}^s(t, \vartheta)) \\ &\quad + \sum_{s=1}^n b_{\ell s} f^s(\bar{\varphi}^s(t, \vartheta)) - \sum_{m=1}^N \xi_m^\ell \sum_{s=1}^n b_{\ell s} f^s(\varphi_m^s(t, \vartheta)) \\ &\quad \left. + \sum_{\eta=1}^{\sigma} \sum_{j=1}^N c^\eta g_{ij}^\eta \gamma_\ell^\eta \varphi_j^\ell(t, \vartheta) + \bar{\mathcal{I}}_i^\ell(t, \vartheta) + u_i^\ell(t, \vartheta) - \sum_{m=1}^N \xi_m^\ell u_m^\ell(t, \vartheta) \right] d\vartheta \\ &\quad + \sum_{i=1}^N \int_a^b \frac{1}{\theta_i} (\kappa_i(t, \vartheta) - \kappa_i^*) \frac{\partial \kappa_i(t, \vartheta)}{\partial t} d\vartheta. \end{aligned} \quad (7)$$

From the Dirichlet boundary condition (2) and applying integration by parts,

$$\sum_{i=1}^N \sum_{\ell=1}^n \xi_i^\ell \int_a^b \varsigma_i^\ell(t, \vartheta) d_\ell \frac{\partial^2 \varsigma_i^\ell(t, \vartheta)}{\partial \vartheta^2} d\vartheta$$

$$= - \int_a^b \left(\frac{\partial \hat{\zeta}(t, \vartheta)}{\partial \vartheta} \right)^T \Lambda(\mathcal{D} \otimes \mathbf{I}_N) \left(\frac{\partial \hat{\zeta}(t, \vartheta)}{\partial \vartheta} \right) d\vartheta. \quad (8)$$

Notice that

$$\sum_{i=1}^N \xi_i^\ell \varsigma_i^\ell(t, \vartheta) = \sum_{i=1}^N \xi_i^\ell \left[\varphi_i^\ell(t, \vartheta) - \sum_{m=1}^N \xi_m^\ell \varphi_m^\ell(t, \vartheta) \right] = 0,$$

which implies that

$$\begin{aligned} & \sum_{i=1}^N \sum_{\ell=1}^n \xi_i^\ell \varsigma_i^\ell(t, \vartheta) \left[\sum_{s=1}^n b_{\ell s} f^s(\bar{\varphi}^s(t, \vartheta)) - \sum_{m=1}^N \xi_m^\ell \sum_{s=1}^n b_{\ell s} f^s(\varphi_m^s(t, \vartheta)) \right] = 0, \\ & \sum_{i=1}^N \sum_{\ell=1}^n \xi_i^\ell \varsigma_i^\ell(t, \vartheta) \left[\sum_{m=1}^N \xi_m^\ell u_m^\ell(t, \vartheta) \right] = 0. \end{aligned}$$

Let

$$\begin{aligned} \tilde{\zeta}_i(t, \vartheta) &= \text{diag}\{\sqrt{\xi_i^n}, \dots, \sqrt{\xi_i^1}\} \varsigma_i(t, \vartheta) \in \mathcal{R}^n, \\ \tilde{F}(\varsigma_i(\cdot, \vartheta)) &= \text{diag}\{\sqrt{\xi_i^n}, \dots, \sqrt{\xi_i^1}\} (f(\varphi_i(\cdot, \vartheta)) - f(\bar{\varphi}(\cdot, \vartheta))) \in \mathcal{R}^n. \end{aligned}$$

From Assumption 1 and Lemma 1,

$$\begin{aligned} & \sum_{\ell=1}^n \varsigma_i^\ell(t, \vartheta) \xi_i^\ell \sum_{s=1}^n b_{\ell s} \left[f^s(\varphi_i^s(t, \vartheta)) - f^s(\bar{\varphi}^s(t, \vartheta)) \right] \\ & \leq \frac{1}{2\varepsilon_1} \sum_{i=1}^N \tilde{\zeta}_i^T(t, \vartheta) \mathcal{B} \mathcal{B}^T \tilde{\zeta}_i(t, \vartheta) + \frac{\varepsilon_1}{2} \sum_{i=1}^N \tilde{F}(\tilde{\zeta}_i^T(t, \vartheta)) \tilde{F}(\tilde{\zeta}_i(t, \vartheta)) \\ & \leq \frac{1}{2} \hat{\zeta}^T(t, \vartheta) \Lambda \left(\frac{1}{\varepsilon_1} \mathcal{B} \mathcal{B}^T \otimes \mathbf{I}_N \right) \hat{\zeta}(t, \vartheta) + \frac{\varepsilon_1 L}{2} \hat{\zeta}^T(t, \vartheta) \Lambda \hat{\zeta}(t, \vartheta). \end{aligned} \quad (9)$$

Along with the controller (5),

$$\begin{aligned} & \sum_{i=1}^N \sum_{\ell=1}^n \int_a^b \varsigma_i^\ell(t, \vartheta) \xi_i^\ell u_i^\ell(t, \vartheta) d\vartheta + \sum_{i=1}^N \int_a^b \frac{1}{\theta_i} (\kappa_i(t, \vartheta) - \kappa^*) \frac{\partial \kappa_i(t, \vartheta)}{\partial t} d\vartheta \\ & = -\kappa^* \sum_{i=1}^N \sum_{\ell=1}^n \int_a^b \xi_i^\ell \varsigma_i^\ell(t, \vartheta) \varsigma_i^\ell(t, \bar{\vartheta}_p) d\vartheta. \end{aligned}$$

Due to $\varsigma_i^\ell(t, \bar{\vartheta}_p) = \varsigma_i^\ell(t, \vartheta) - \int_{\bar{\vartheta}_p}^{\vartheta} \frac{\partial \varsigma_i^\ell(t, s)}{\partial s} ds$, $\vartheta_{p+1} - \bar{\vartheta}_p \leq \frac{\delta}{2}$ and $\bar{\vartheta}_p - \vartheta_p \leq \frac{\delta}{2}$, in view of Lemmas 1, 2,

$$-\kappa^* \sum_{i=1}^N \sum_{\ell=1}^n \int_a^b \xi_i^\ell \varsigma_i^\ell(t, \vartheta) \varsigma_i^\ell(t, \bar{\vartheta}_p) d\vartheta$$

$$\begin{aligned}
&= -\kappa^* \int_a^b \zeta^T(t, \vartheta) \Lambda \hat{\zeta}(t, \vartheta) d\vartheta + \kappa^* \int_a^b \zeta^T(t, \vartheta) \Lambda \left(\int_{\bar{\vartheta}_p}^{\vartheta} \frac{\partial \hat{\zeta}(t, s)}{\partial s} ds \right) d\vartheta \\
&\leq -\kappa^* \int_a^b \zeta^T(t, \vartheta) \Lambda \hat{\zeta}(t, \vartheta) d\vartheta + \kappa^* \frac{\varepsilon_2}{2} \sum_{p=0}^{m-1} \int_{\vartheta_p}^{\vartheta_{p+1}} \zeta^T(t, \vartheta) \Lambda \hat{\zeta}(t, \vartheta) d\vartheta \\
&\quad + \kappa^* \frac{1}{2\varepsilon_2} \sum_{p=0}^{m-1} \left[\int_{\vartheta_p}^{\bar{\vartheta}_p} \left(\hat{\zeta}(t, \vartheta) - \hat{\zeta}(t, \bar{\vartheta}_p) \right)^T \Lambda \left(\hat{\zeta}(t, \vartheta) - \hat{\zeta}(t, \bar{\vartheta}_p) \right) d\vartheta \right. \\
&\quad \left. + \int_{\bar{\vartheta}_p}^{\vartheta_{p+1}} \left(\hat{\zeta}(t, \vartheta) - \hat{\zeta}(t, \bar{\vartheta}_p) \right)^T \Lambda \left(\hat{\zeta}(t, \vartheta) - \hat{\zeta}(t, \bar{\vartheta}_p) \right) d\vartheta \right] \\
&\leq -\kappa^* \left(1 - \frac{\varepsilon_2}{2}\right) \int_a^b \zeta^T(t, \vartheta) \Lambda \hat{\zeta}(t, \vartheta) d\vartheta \\
&\quad + \kappa^* \frac{\delta^2}{2\varepsilon_2 \pi^2} \int_a^b \left(\frac{\partial \hat{\zeta}(t, \vartheta)}{\partial \vartheta} \right)^T \Lambda \left(\frac{\partial \hat{\zeta}(t, \vartheta)}{\partial \vartheta} \right) d\vartheta. \tag{10}
\end{aligned}$$

Substituting formulas (8)-(10) into (7) yields,

$$\begin{aligned}
-\hat{\psi}_1(t) &\leq \int_a^b \zeta^T(t, \vartheta) \tilde{\Upsilon} \hat{\zeta}(t, \vartheta) d\vartheta + \int_a^b \zeta^T(t, \vartheta) \left(\frac{1}{2} \Lambda + \mathcal{P}^T [\mathcal{H}_2]^s \mathcal{Q} - \frac{1}{2} \mathcal{H}^T \mathcal{P} \right) \hat{\mathcal{I}}(t, \vartheta) d\vartheta \\
&\quad + \int_a^b \hat{\mathcal{I}}^T(t, \vartheta) \left(\frac{1}{2} \Lambda + \mathcal{Q}^T [\mathcal{H}_2]^s \mathcal{P} - \frac{1}{2} \mathcal{H}^T \mathcal{P} \right) \hat{\zeta}(t, \vartheta) d\vartheta \\
&\quad + \int_a^b \hat{\mathcal{I}}^T(t, \vartheta) d\vartheta \left(\mathcal{Q}^T [\mathcal{H}_2]^s \mathcal{Q} + [\mathcal{H}_1]^s - [\mathcal{Q}^T \mathcal{H}]^s \right) \hat{\mathcal{I}}(t, \vartheta) d\vartheta \\
&\quad + \int_a^b \left(\frac{\partial \hat{\zeta}(t, \vartheta)}{\partial \vartheta} \right)^T \Lambda \left[\left(\frac{\kappa^* \delta^2}{2\varepsilon_2 \pi^2} \mathbf{I}_n - \mathcal{D} \right) \otimes \mathbf{I}_N \right] \left(\frac{\partial \hat{\zeta}(t, \vartheta)}{\partial \vartheta} \right) d\vartheta \\
&= \int_a^b \tilde{\mathbf{E}}^T(t, \vartheta) \Omega \tilde{\mathbf{E}}(t, \vartheta) d\vartheta,
\end{aligned}$$

where $\tilde{\mathbf{E}}(t, \vartheta) = \left(\hat{\zeta}(t, \vartheta), \hat{\mathcal{I}}(t, \vartheta), \frac{\partial \hat{\zeta}(t, \vartheta)}{\partial t} \right)^T$, $\tilde{\Upsilon} = -\mathcal{P}^T \mathcal{H}_2 \mathcal{P} + [\Lambda \mathcal{G}]^s - \Lambda \left[\left(\mathcal{A} - \frac{\mathcal{B} \mathcal{B}^T}{2\varepsilon_1} - \frac{\varepsilon_1 L}{2} \mathbf{I}_n \right) \otimes \mathbf{I}_N + \kappa^* \left(1 - \frac{\varepsilon_2}{2}\right) \right]$,

$$\begin{aligned}
\Omega &= \begin{pmatrix} \tilde{\Upsilon} & \Omega_{12} & 0 \\ \Omega_{12}^T & \Omega_{22} & 0 \\ 0 & 0 & \Omega_{33} \end{pmatrix}, \quad \Omega_{12} = \frac{1}{2} \Lambda + \mathcal{P}^T [\mathcal{H}_2]^s \mathcal{Q} - \frac{1}{2} \mathcal{H}^T \mathcal{P}, \\
\Omega_{22} &= \mathcal{Q}^T [\mathcal{H}_2]^s \mathcal{Q} + [\mathcal{H}_1]^s - [\mathcal{Q}^T \mathcal{H}]^s, \quad \Omega_{33} = \Lambda \left[\left(\frac{\kappa^* \delta^2}{2\varepsilon_2 \pi^2} \mathbf{I}_n - \mathcal{D} \right) \otimes \mathbf{I}_N \right].
\end{aligned}$$

By selecting κ^* such that $\Omega \leq 0$, one has $\hat{\psi}_1(t) \geq 0$. \square

Corollary 1. Under Assumptions 1-2 and the adaptive spatial sampling controller (5), there exist matrices $\mathcal{H} \in \mathcal{R}^{pN \times nN}$ and $0 < \mathcal{H}_1 \in \mathcal{R}^{pN \times pN}$ such

that system (3) is output-strictly passive. Moreover, there exist matrices $\mathcal{H} \in \mathcal{R}^{pN \times nN}$ and $0 < \mathcal{H}_2 \in \mathcal{R}^{nN \times nN}$ such that system (3) is input-strictly passive.

3.2 Passive-based synchronization

Definition 2. The spatiotemporal neural network (1) is asymptotically synchronized if

$$\lim_{t \rightarrow +\infty} \|\hat{\zeta}(t, \vartheta)\|_{[a,b]} = 0.$$

Theorem 2. Under Assumptions 1-2 and adaptive spatial sampling controller (5), the spatiotemporal neural network (1) with $\hat{\mathcal{I}}(t, \vartheta) = \mathbf{0}_{nN}$ is asymptotically synchronized if the error system (3) is output-strictly passive and $P^T \mathcal{H}_2 P > 0$. **Proof.** Picking the same Lyapunov function $W(t)$ as Theorem 1. Under the adaptive controller (5), the error system (3) is output-strictly passive which obtained by Corollary 1 that

$$\dot{W}(t) \leq \int_a^b \hat{\mathcal{O}}^T(t, \vartheta) \mathcal{H} \hat{\mathcal{I}}(t, \vartheta) d\vartheta - \int_a^b \hat{\mathcal{O}}^T(t, \vartheta) \mathcal{H}_2 \hat{\mathcal{O}}(t, \vartheta) d\vartheta$$

When $\hat{\mathcal{I}}(t, \vartheta) = \mathbf{0}_{nN}$ and $P^T \mathcal{H}_2 P > 0$,

$$\dot{W}(t) \leq - \int_a^b \hat{\zeta}^T(t, \vartheta) P^T \mathcal{H}_2 P \hat{\zeta}(t, \vartheta) d\vartheta \leq -\lambda_{\min}(P^T \mathcal{H}_2 P) \int_a^b \hat{\zeta}^T(t, \vartheta) \hat{\zeta}(t, \vartheta) d\vartheta < 0. \quad (11)$$

which means that $W(t)$ is bounded.

Next, the fact $\lim_{t \rightarrow \infty} \int_a^b \hat{\zeta}^T(t, \vartheta) \hat{\zeta}(t, \vartheta) d\vartheta = 0$ will be proved. If this is not true, assume that there exists a $\mu > 0$ satisfying $\lim_{t \rightarrow \infty} \int_a^b \hat{\zeta}^T(t, \vartheta) \hat{\zeta}(t, \vartheta) d\vartheta = \mu$. Then, there exists a real number $M > 0$ such that

$$\int_a^b \hat{\zeta}^T(t, \vartheta) \hat{\zeta}(t, \vartheta) d\vartheta > \frac{\mu}{2}, \quad t \geq M.$$

From (11),

$$\dot{W}(t) \leq -\lambda_{\min}(P^T \mathcal{H}_2 P) \int_a^b \hat{\zeta}^T(t, \vartheta) \hat{\zeta}(t, \vartheta) d\vartheta \leq -\frac{\mu \lambda_{\min}(P^T \mathcal{H}_2 P)}{2}, \quad t \geq M. \quad (12)$$

By integrating (12) with respect to t over M to ∞ ,

$$-W(M) \leq W(+\infty) - W(M) < - \int_M^{\infty} \frac{\mu \lambda_{\min}(P^T \mathcal{H}_2 P)}{2} dt = -\infty,$$

which is inconsistent with the boundedness of $W(t)$. Therefore, $\lim_{t \rightarrow \infty} \|\hat{\zeta}(t, \cdot)\|_{[a,b]} = 0$.

The proof is completed. \square

4 Numerical Simulations

Consider a kind of spatiotemporal neural networks (1) with 3-weighted couplings, where $t \in \mathcal{R}_{\geq 0}$, $\vartheta \in (0, 10)$, $\mathcal{D} = 0.6\mathbf{I}_3$, $\mathcal{A} = 0.7\mathbf{I}_3$, $f(\varphi) = \tanh(\varphi)$, $c^1 = c^3 = 0.15$, $c^2 = 0.25$, $\Gamma^1 = \text{diag}\{0.1, 0.2, 0.1\}$, $\Gamma^2 = \text{diag}\{0.25, 0.2, 0.3\}$, $\Gamma^3 = \text{diag}\{0.25, 0.1, 0.3\}$, $\vartheta \in [0.1p, 0.1(p+1)]$ ($p \in \overline{0, 99}$), the boundary $\varphi_i(0, 0) = \varphi_i(0, 10) = \mathbf{0}_3$, initial conditions $\phi(\vartheta)$ are given as arbitrary constants in $[-50, 50]$ for $\vartheta \in (0, 10)$, The output and input vectors are defined as $\mathcal{O}_i(t, \vartheta) = P\varsigma_i(t, \vartheta) + Q\mathcal{I}_i(t, \vartheta)$, $i \in \overline{1, 5}$, where $P = 5\mathbf{I}_3$ and $Q = 2\mathbf{I}_3$, and $\mathcal{I}_i(t, \vartheta) = [0.05i \sin(\frac{\pi}{2} + x) \cos(0.05t), 0.1i \sin(\frac{\pi}{2} + x) \cos(0.01t), 0.15i \sin(\frac{\pi}{2} + x) \cos(0.01t)]^T$,

$$B_1 = \begin{bmatrix} 3 & 12 & 21 \\ -15 & 3 & 3.6 \\ -27 & 12 & -1.8 \end{bmatrix}.$$

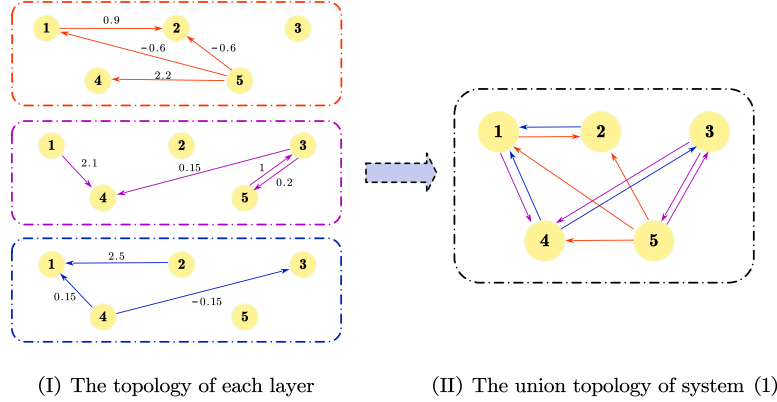


Fig. 1. The joint connectivity

It follows that the topology of system (1) is illustrated in Fig. 1, the weighted union communication topology is strongly connected. A straightforward calculation yields $L = 1$, and the vectors $\xi^{(1)} = \xi^{(2)} = \xi^{(3)} = 0.2\mathbf{1}_5$ satisfy $(G^{(1)})^T \xi^{(1)} = (G^{(2)})^T \xi^{(2)} = (G^{(3)})^T \xi^{(3)} = \mathbf{0}_5$.

Case 1. Choose $\varepsilon_1 = 8.5$, $\varepsilon_2 = 1$ and $\theta_i = 4.7$ ($i \in \overline{1, 5}$),

$$\mathcal{H} = \begin{bmatrix} 0.5229 & 0.0464 & 0.0176 \\ 0.0464 & 0.2813 & 0.3027 \\ 0.0176 & 0.3027 & 0.7195 \end{bmatrix} \otimes \mathbf{I}_5, \quad \mathcal{H}_1 = \begin{bmatrix} 0.1269 & -1.2810 & -0.4847 \\ 1.3019 & 0.0727 & -8.3579 \\ 0.4926 & 8.4937 & 0.1710 \end{bmatrix} \otimes \mathbf{I}_5,$$

$$\mathcal{H}_2 = \begin{bmatrix} 0.2677 & -0.0744 & -0.0282 \\ 0.1261 & 0.1330 & -0.4855 \\ 0.0477 & 0.8230 & 0.3773 \end{bmatrix} \otimes \mathbf{I}_5.$$

Under the adaptive spatial sampling controller (5), from Theorem 1, the strict passivity of error system (3) is realized and shown in Fig. 2 and Fig. 3.

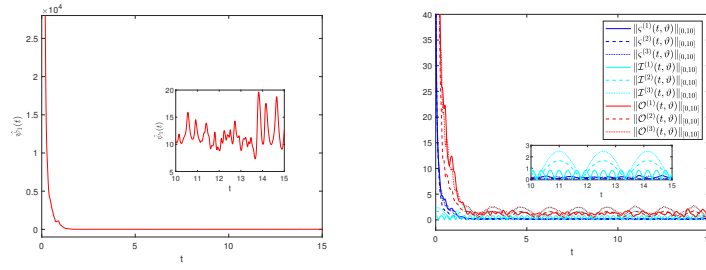


Fig. 2. Evolution of function $\hat{\psi}(t, \vartheta)$ and error $\zeta(t, \vartheta)$ in Case 1

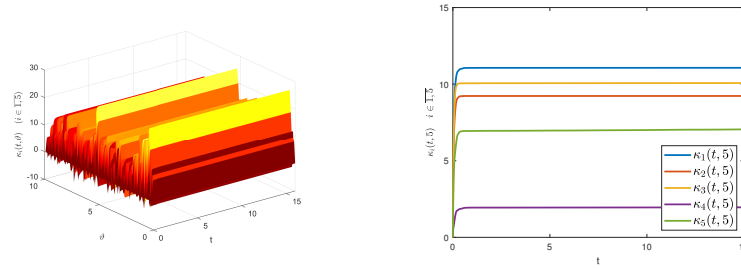


Fig. 3. Spatiotemporal evolution of control gain κ changes in Case 1

Case 2. Choose $\varepsilon_1 = 8.5$, $\varepsilon_2 = 1$ and $\theta_i = 4.7$ ($i \in 1, 5$),

$$\mathcal{H} = \begin{bmatrix} 0.5242 & 0.0462 & 0.0175 \\ 0.0462 & 0.2834 & 0.3016 \\ 0.0175 & 0.3016 & 0.7200 \end{bmatrix} \otimes \mathbf{I}_5, \mathcal{H}_2 = \begin{bmatrix} 0.2691 & 0.0267 & 0.0099 \\ 0.0250 & 0.1345 & 0.1694 \\ 0.0097 & 0.1680 & 0.3786 \end{bmatrix} \otimes \mathbf{I}_5.$$

Under the adaptive spatial sampling controller (5), from Corollary 1, the output-strict passivity of error system (3) is realized and shown in Fig. 4 and Fig. 5.

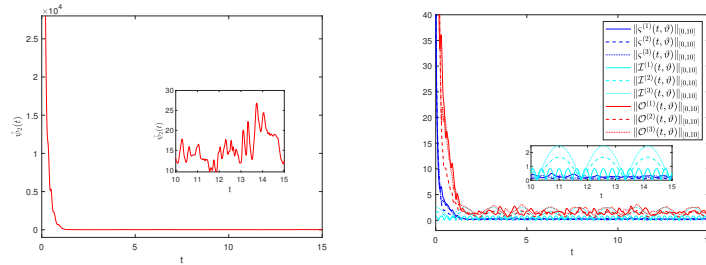


Fig. 4. Evolution of function $\hat{\psi}(t, \vartheta)$ and error $\zeta(t, \vartheta)$ in Case 2

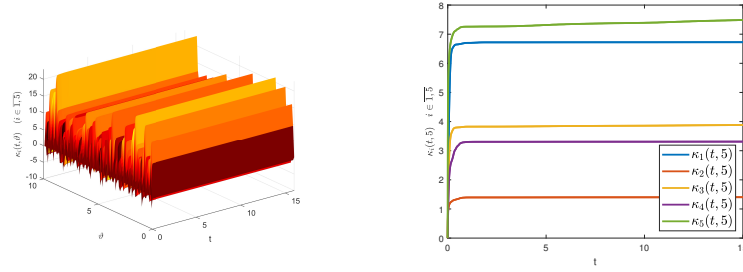


Fig. 5. Spatialtemporal evolution of control gain κ changes in Case 2

Case 3. Let $\varepsilon_1 = 7$, $\varepsilon_2 = 1$ and $\theta_i = 5$ ($i \in 1, 5$),

$$\mathcal{H} = \begin{bmatrix} 0.1240 & -0.0086 & -0.0038 \\ -0.0086 & 0.1654 & -0.0570 \\ -0.0038 & -0.0570 & 0.0830 \end{bmatrix} \otimes \mathbf{I}_5, \mathcal{H}_1 = \begin{bmatrix} 0.0352 & -75.1595 & -120.6295 \\ 75.1554 & 0.0457 & -485.5432 \\ 120.6279 & 485.5163 & 0.0262 \end{bmatrix} \otimes \mathbf{I}_5.$$

Under the spatial sampled-data controller (5), from Corollary 1, the input-strict passivity of error system (3) is realized and shown in Fig. 6 and Fig. 7.

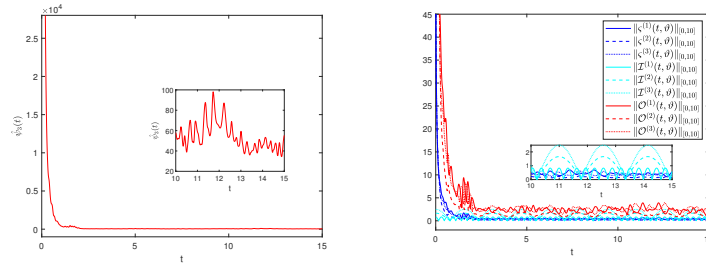


Fig. 6. Evolution of function $\hat{\psi}(t, \vartheta)$ and error $\zeta(t, \vartheta)$ in Case 3

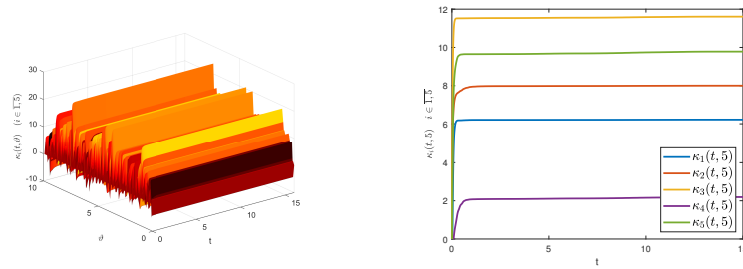


Fig. 7. Spatialtemporal evolution of control gain κ changes in Case 3

Next, the adaptive passivity-based synchronization of the spatiotemporal neural networks (1) is verified. Fig. 8 shows that the spatiotemporal neural networks (1) fails to achieve synchronization without control. Under the adaptive

spatial sampling controller (5), the error system (3) is output-strictly passive in Case 2. When $\tilde{\mathcal{L}}(t, \vartheta) = \mathbf{0}_{15}$, the system (1) is synchronized through Theorem 2, which is illustrated by Fig. 9.

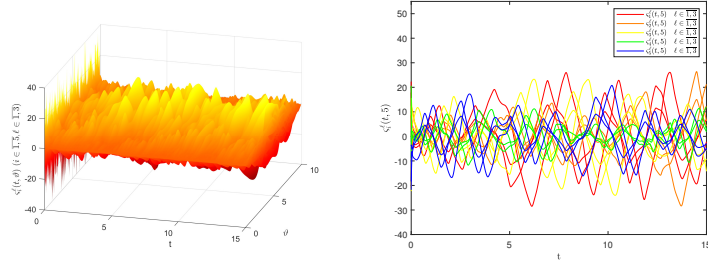


Fig. 8. Spatiotemporal evolution of $\zeta_i^\ell(t, \vartheta)$ without control

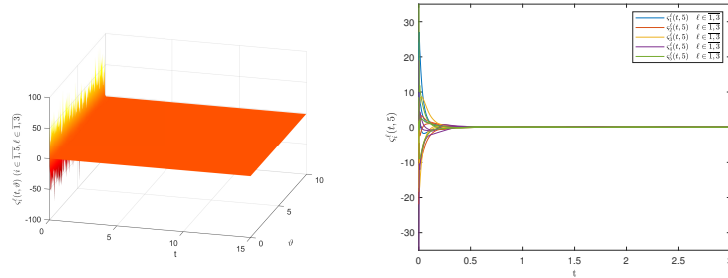


Fig. 9. Synchronization evolution under the adaptive spatial sampling controller (5)

5 Conclusion

This paper investigates the passivity and synchronization of spatiotemporal neural networks with multi-weight coupling via adaptive spatial sampling control. The proposed strategy integrates spatial sampling and adaptive control, reducing control costs and enhancing practical applicability. By constructing an appropriate Lyapunov function and utilizing variable rearrangement techniques with passivity theory, several passivity and synchronization criteria are derived. Numerical simulation is conducted to verify the effectiveness of the theoretical results. Future research will explore finite-time passive synchronization of spatiotemporal neural networks under adaptive spatial sampling control.

References

1. Liu, X.W.: Synchronization and control for multiweighted and directed complex networks. *IEEE Trans. Neural Netw. Learn. Syst.* 34, 3226–3233 (2023)
2. Lin, S.R., Liu, X.W.: Robust passivity and control for directed and multiweighted coupled dynamical networks. *IEEE Trans. Neural Netw. Learn. Syst.* 34(12), 10458–10472 (2023)

3. Yao, Q., Lin, P., Wang, L.S., Wang, Y.F.: Practical exponential stability of impulsive stochastic reaction-diffusion systems with delays. *IEEE Trans. Cybern.* 52(5), 2687–2697 (2022)
4. Zhao, L.H., Wen, S., Zhu, S., Guo, Z., Huang, T.: Robust pinning synchronization for multiweighted coupled reaction-diffusion neural networks. *IEEE Trans. Cybern.* 53(10), 6549–6561 (2023)
5. Bevelevich, V.: *Classical Network Synthesis*. Van Nostrand, New York (1968)
6. Willems, J.C.: Dissipative dynamical systems-Part I: General theory. *Arch. Ration. Mech. Anal.* 45(5), 321–351 (1972)
7. Wang, J.L.: Passivity for multiadaptive coupled fractional-order reaction-diffusion neural networks. In: *Dynamical Behaviors of Fractional-Order Complex Dynamical Networks*, pp. 141–168. Springer, Singapore (2024)
8. Huang, Y.L., Lin, S.R., Yang, E.F.: Event-triggered passivity of multi-weighted coupled delayed reaction-diffusion memristive neural networks with fixed and switching topologies. *Commun. Nonlinear Sci. Numer. Simul.* 89, Art. no. 105292 (2020)
9. Wang, Y.H.: Event-triggered passivity and synchronization of multiple derivative coupled reaction-diffusion neural networks. *Neurocomputing* 586, Art. no. 127619 (2024)
10. Wang, J.L., Zhao, L.H.: PD and PI control for passivity and synchronization of coupled neural networks with multi-weights. *IEEE Trans. Netw. Sci. Eng.* 8, 790–802 (2021)
11. Fan, H.G., Chen, X.J., Shi, K.B., Wen, H.: Distributed delayed impulsive control for μ -synchronization of multi-link structure networks with bounded uncertainties and time-varying delays of unmeasured bounds: A novel Halanay impulsive inequality approach. *Chaos Solitons Fractals* 186, Art. no. 115226 (2024)
12. Hou, J., Huang, Y.L., Wang, J.L., Ren, S.Y., Liu, D.F.: Anti-synchronization analysis and pinning control of coupled neural networks with multiple weights. In: *Proc. 2018 IEEE 8th Annu. Int. Conf. CYBER Technol. Autom. Control Intell. Syst.*, pp. 895–900 (2018)
13. Nie, H., Zhang, Y.: Finite-time cluster synchronization of multi-weighted fractional-order coupled neural networks with and without impulsive effects. *Neural Netw.* 180, Art. no. 106646 (2024)
14. Yang, S.Y., Tang, H.A., Hu, X., Xia, Q., Wang, L., Duan, S.: Adaptive finite-time passivity and synchronization of coupled fractional-order memristive neural networks with multi-state couplings. *Neurocomputing* 579, Art. no. 127380 (2024)
15. Wang, J.L., Zhu, Y.R., Wang, J.Q., Ren, S.Y., Huang, T.: Adaptive event-triggered lag outer synchronization for coupled neural networks with multistate or multiderivative couplings. *IEEE Trans. Cybern.* 55(3), 1018–1031 (2025)
16. Sun, Y., Hu, C., Wen, S.P., Yu, J., Jiang, H.J.: Pinning adaptive passivity and bipartite synchronization of leaderless fractional spatiotemporal networks. *IEEE Trans. Netw. Sci. Eng.* 12, 319–331 (2025)
17. Cao, Y.T., Zhao, L.H., Zhong, Q.H., Wen, S.P., Shi, K.B., Xiao, J.Y., Huang, T.W.: Adaptive fixed-time output synchronization for complex dynamical networks with multi-weights. *Neural Netw.* 163, 28–39 (2023)
18. Liu, X.Z., Wu, K.N., Zhang, W.H.: Mean square finite-time boundary stabilisation and H_∞ boundary control for stochastic reaction-diffusion systems. *Int. J. Syst. Sci.* 50, 1388–1398 (2019)
19. Liu, K., Fridman, E.: Wirtinger’s inequality and Lyapunov-based sampled-data stabilization. *Automatica* 48(1), 102–108 (2012)